# 2.18 Development of Fe-based HTS Wire and Conceptual Design Study of the Magnet for Future High Energy Accelerators

Chao Yao and Yanwei Ma
Mail to: ywma@mail.iee.ac.cn
Key Laboratory of Applied Superconductivity, Institute of Electrical Engineering, Chinese Academy of Sciences, Beijing 100190, China

Ershuai Kong, Chengtao Wang and Qingjin Xu
Mail to: xuqj@ihep.ac.cn
Accelerator Division, Institute of High Energy Physics, Chinese Academy of Sciences, Beijing 100049, China

## 2.18.1 Introduction

Iron-based superconductors (IBSs) discovered in 2008 formed the second high-$T_c$ superconductor family after cuprate superconductors, and have aroused extensive research for their physical nature and application potential [1,2]. According to different chemical compositions and crystal structures, IBSs can be categorized into several types, such as '1111' type (e.g. $LaFeAsO_{1-x}F_x$ and $SmFeAsO_{1-x}F_x$), '122' type (e.g. $Ba_{1-x}K_xFe_2As_2$ and $Sr_{1-x}K_xFe_2As_2$), '111' type (e.g. LiFeAs) and '11' type (e.g. FeSe, $FeSe_{1-x}Te_x$). IBSs have very high upper critical fields ($H_{c2}$) above 100 T, small electromagnetic anisotropy (1.5-2 for '122' IBS), relatively high superconducting transition temperatures ($T_c$) (up to 38 K for '122' IBS and 56 K for '1111' IBS), and large critical current density ($J_c$) over $10^6$ A/cm$^2$ in thin films. Nowadays, high-field magnets are one of the most important aspects for the applications of high-$T_c$ superconductors, so $H_{c2}$ is a key property we must concern about. As shown in Figure 1, the conventional low-$T_c$ superconductors (NbTi and $Nb_3Sn$) restrict the magnets with field below 25 T at liquid helium temperature. For '122' and '1111' IBS, the $H_{c2}$ is much higher than that of low-$T_c$ superconductors, and is still above 40 T at 20 K. In addition to its low anisotropy, IBS is quite attractive for the construction of high-field magnets, which are desired for the next generation of NMR, accelerator, and fusion magnets, and can work at liquid helium temperature and also in moderate temperature range around 20 K, which can be obtained by cryocoolers.

Studies on the grain boundary nature in '122' IBS epitaxial film suggested that intergrain currents across mismatched grains in iron-based superconductors are deteriorated to a lesser extent than in YBCO superconductors [4]. Therefore, the low-cost powder-in-tube (PIT) method, which has been utilized in commercial $Nb_3Sn$、Bi-2223 and $MgB_2$ wires, is promising for IBS wires manufacture. On the other hand, in contrast to BiSrCaCuO wires, whose sheath material was limited to silver or some silver rich alloys due to the oxygen permeability for sheath material, the IBS wires have more choices for sheath materials. Though silver is the most widely used sheath material for 1111- and 122-type IBS wires at present, since it is chemically stable and not easy to react with IBS phase during heat treatment of IBS wires, using other cheap and stiff metal material as the outer sheath for IBS/Ag composite conductors can be a practical proposal to reduce the ratio of silver cost, provide sheath chemical stability, and enhance mechanical properties at the same time. Therefore, the low-cost, high-strength and high $J_c$ performance IBS wire and tape conductors are very promising based on PIT method.

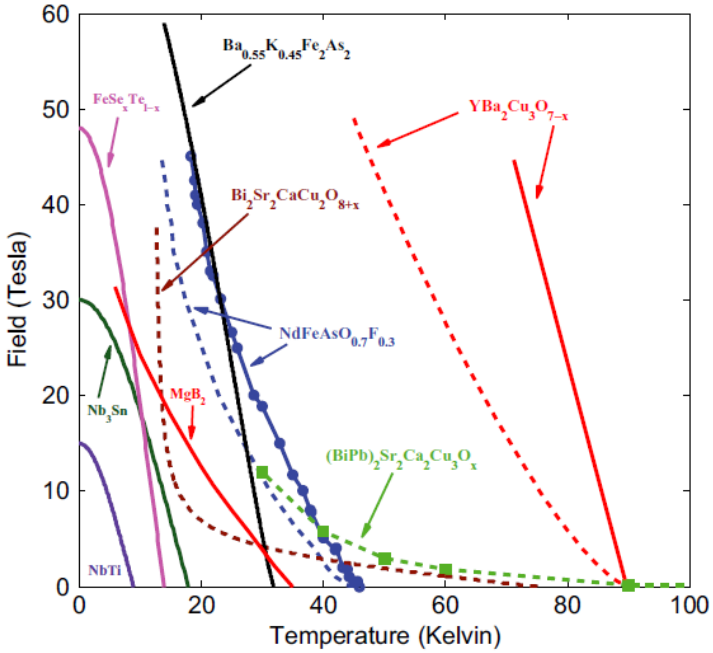


**Figure 1:** Comparative T-H phase diagram for different superconducting materials. Here the solid and dashed lines show the upper critical field $H_{c2}(T)$ and the irreversibility fields $H^*(T)$ for H//c, respectively [3].

A conceptual design study of 12-T 2-in-1 dipole magnets is ongoing with the Iron-based superconducting (IBS) technology, to fulfill the requirements and need of a proposed large-scale superconducting accelerator: Super Proton Proton Collider (SPPC), which aims to discover the new physics beyond the standard model with a 100-km circumference tunnel and 70 TeV center-of-mass energy. The design study is carried out with an expected $J_e$ level of IBS in 10 years, i.e., about 10 times higher than the present level. Besides the significant improvement of $J_e$, we are also expecting that the IBS superconductor would have much better mechanical performance comparing with present high field conductors like $Nb_3Sn$, ReBCO and Bi-2212, and the much lower cost than them.

The aperture diameter of the magnets is 45 mm. The main field is 12 T in the two apertures per magnet with $10^{-4}$ field uniformity. The common-coil configuration is adopted for the coil layout because of its simple structure and easy to fabricate. Two types of coil ends are considered and compared for the field quality and structure optimization: soft-way bending and hard-way bending. For the hard-way bending the coil is wound with flared ends and in such way the needed superconductors is minimized. The main parameters, coil layouts and the field quality optimization of this design study will be presented.

### 2.18.2 **Development of Advanced IBS HTS Wire**

IBS wire and tape conductors with high transport current density are essential for practical applications. In 2008, the first iron-based superconducting wires are developed in Institute of Electrical Engineering, Chinese Academy of Sciences (IEECAS) by *in-situ* powder-in-tube (PIT) method, which starts by packing the powders of unreacted precursor materials into a metallic tube in a high purity Ar atmosphere. However, the

defects in the material such as micro cracks, low density, phase inhomogeneity, and impurity phase still restricted the transport current in wires. By using *ex-situ* PIT method, in which reacted and well ground superconducting materials are packed into metallic tubes, the mass density and phase homogeneity of the wire after the final heat treatment are significantly improved in '1111' and '122' IBS wires [5].

In the recent years, mechanical deformation processes such as flat rolling, hot isostatic pressing and uniaxial pressing have significantly improved the mass density of superconducting phase, resulting in a dramatic increase for the transport $J_c$ of 122-type IBS wires and tapes. In 2012, the Florida State University achieved a transport $J_c$ of $8.5\times10^3$ A/cm$^2$ at 4.2 K and 10 T in Cu/Ag clad $Ba_{1-x}K_xFe_2As_2$ (Ba-122) wires, which were processed using a hot isostatic press technique (HIP) and low-temperature sintering to obtain high mass density and fine grains [6]. With a further optimized HIP process, the transport $J_c$ for Ba-122 round wires were recently increased to $2\times10^4$ A/cm$^2$ at 4.2 K and 10 T by the University of Tokyo [7]. Using combination process of cold flat rolling and uniaxial pressing, which can increase the density of superconducting cores and change in the microcrack structure, high transport $J_c$ of $8.6\times10^4$ A/cm$^2$ at 4.2 K and 10 T were obtained in silver sheathed Ba-122 tapes in National Institute for Materials Science (NIMS) [8]. In 2014, researchers in IEECAS processed the as-rolled $Sr_{1-x}K_xFe_2As_2$ (Sr-122) tapes by a hot press technique, which significantly increased the mass density of the superconducting core, and eliminated the residual micro-cracks induced during the defamation process, thus improving the transport $J_c$ to practical level of $10^5$ A/cm$^2$ (4.2 K, 10 T) for the first time [9].

In addition to the material defects mentioned above, the high-angle grain boundary in iron pnictides also deteriorated the transport currents, so the misoriented grains should be improved to further enhance the $J_c$ performance for IBS wires and tapes. In 2011, IEECAS first reported c-axis textured Sr-122 tapes with Fe sheath by flat rolling. Recently, by using optimized hot press process to achieved a higher degree of grain texture, the transport $J_c$ was further increase to $1.5\times10^5$ A/cm$^2$ ($I_c$ = 437 A) at 4.2 K and 10 T in Ba-122 tapes, as shown in Figure 2. The transport $J_c$ measured at 4.2 K under high magnetic fields of 27 T is still on the level of $5.5\times10^4$ A/cm$^2$. Moreover, at 20 K and 5 T the transport $J_c$ is also as high as $5.4\times10^4$ A/cm$^2$, showing a great application potential in moderate temperature range which can be reached by liquid hydrogen or cryogenic cooling [10].

The mechanical properties of wires and tapes is another important issue, since conductor strength and its tolerance to the mechanical load are quite crucial for practical application, especially for operations under high magnetic field. By using a U-shaped bending spring (U-spring) method, the compressive strain dependence of transport $J_c$ for silver sheathed '122' IBS tapes was investigated. Reversible $J_c$ performance under lager compressive strain of -0.6% in high magnetic field of 10 T was observed. This result demonstrates the great potential of '122' IBS for high-field application, in which conductors are designed to work under compression strain for safety [11].

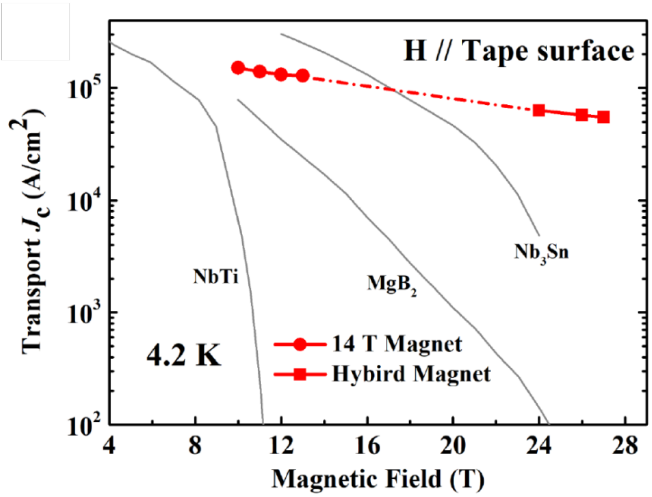


**Figure 2:** The field dependence of transport $J_c$ values at 4.2 K for hot pressed Sr-122 tapes, compared with commercial NbTi, $Nb_3Sn$ and $MgB_2$ wires.

For practical applications of iron-based superconductors, fabricating wires and tapes with multifilaments in metal matrix to protect against flux jumps and thermal quenching is an important step. Based on the techniques used in the single-core IBS wires, Ag/Fe clad 7-filament Sr-122 wires and tapes were successfully fabricated in IEECAS in 2013 [12]. After that, Ag/Fe sheathed 114-filament Sr-122/Fe wires and tapes were also produced, as shown in Figure 3. Processed with hot press, a high transport $J_c$ of $3.6\times10^4$ A/cm$^2$ at 4.2 K and 10 T can be achieved in 7-filament Sr-122/Monel tapes, which exhibits an improved mechanical strength and very weak field dependence for transport $J_c$. In addition, using copper instead of expensive silver as sheath material was attempted for Sr-122 tapes. By shortening the time of heat treatment to control the reaction between sheath material and IBS core, a high transport $J_c$ of $3.5\times10^4$ A/cm$^2$ and $1.6\times10^4$ A/cm$^2$ was achieved at 4.2 K, 10 T and 26 T in Cu-sheathed Sr-122 tapes, respectively [13]. This result is very significant for fabricating high-performance and low-cost IBS wires, since copper is cost effective, has good mechanical properties, and can provides reliable thermal stabilization in practical applications.

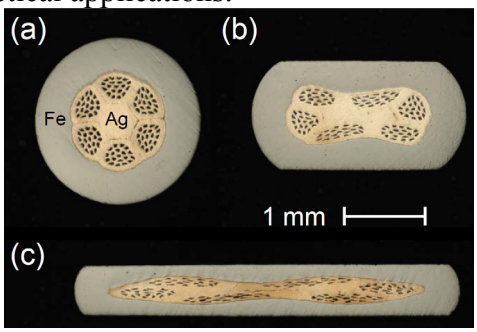


**Figure 3**: Optical images of the transverse cross section for 114-filament Sr-122/Ag/Fe **(a)** wires of 2.0mm in diameter and tapes of **(b)** 1.0mm and **(c)** 0.6mm in thickness.

Though high $J_c$ properties can be obtained in short '122' IBS samples, practical applications need wire and tape conductors with sufficient length. In 2014, the IEECAS group fabricated the first 11 m long Sr-122/Ag tape by a scalable rolling process. The $J_c$

of this tape exhibits a uniform distribution, fluctuating between 2.12 and $1.68\times10^4$ A/cm$^2$ (4.2 K, 10 T), with an average $J_c$ value of $1.84\times10^4$ A/cm$^2$ [14]. After carefully optimizing the long-length wire fabricating process to achieve a higher-level uniformity of deformation, the world's first 100 meter-class IBS tapes was produced by the same group [15]. As presented in Figure 4, this 115 m long 7-filament Sr-122/Ag tape shows a uniform $J_c$ distribution throughout the tape with a minimum $J_c$ of $1.2\times10^4$ A/cm$^2$ (4.2 K, 10 T), demonstrating great potential in large-scale manufacture and a promising future of iron-based superconductors for practical applications. In the future, by further optimizing the wire architecture, cold work process and heat treatment parameters, it can be expected that the high $J_c$ performance in short IBS samples to be realized in high-strength long-length multifiamentary IBS wires, which are desirable for high-field applications.

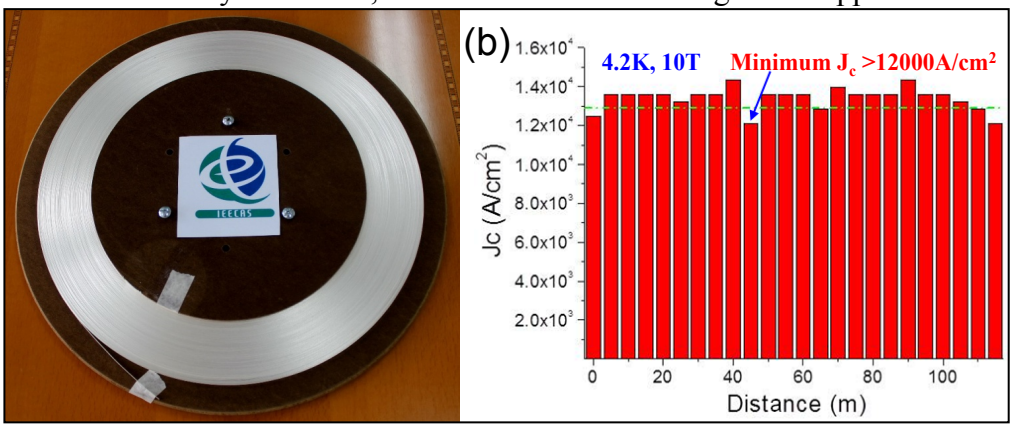


**Figure 4**: **(a)** World's first 100 meter-class iron-based superconducting wire developed in Institute of Electrical Engineering, Chinese Academy of Sciences (IEECAS), and **(b)** the distribution of critical current density $J_c$ throughout the wire.

### 2.18.3 Conceptual Design Study of the Dipole Magnet for Future High Energy Accelerators

SPPC needs thousands of 12~24 T (upgrading phase) dipole and quadrupole magnets to bend and focus proton beams [16, 17]. The nominal aperture in these magnets is 40~50 mm. A field uniformity of $10^{-4}$ should be attained in up to 2/3 of the aperture radius. The magnets will have two beam apertures of opposite magnetic polarity within the same yoke to save space and cost. The currently assumed distance between the two apertures in the main dipoles is 200~300 mm, but this could be changed based on the detailed design optimization to control cross-talk between the two apertures, and with considerations on the overall magnet size. The outer diameter of the main dipole and quadrupole magnets should not be larger than 900 mm, so that they can be placed inside cryostats having an outer diameter of 1500 mm. The total magnetic length of the main dipole magnets is about 65.4 km out of the total circumference of 100 km. If the length of each dipole magnet is about 15 m, then about 4360 dipole magnets are required.

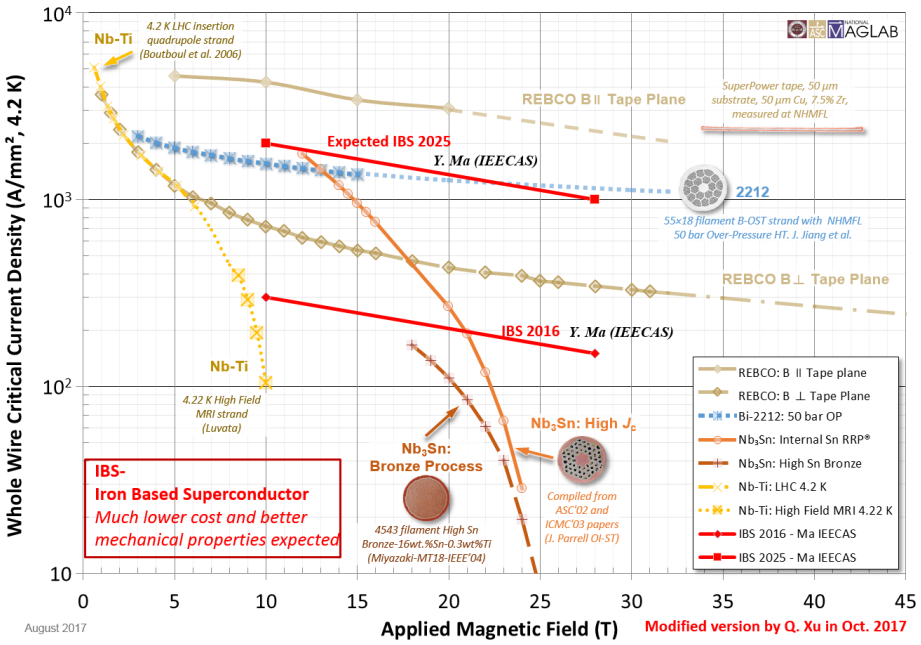


**Figure 5**: $J_e$ of IBS in 10 years comparing with other practical materials

All the superconducting magnets used in present accelerators are based on NbTi technology. These magnets work at significantly lower field than the required 12~24 T, e.g., 3.5 T at 4.2 K at RHIC and 8.3 T at 1.9 K at LHC [18, 19]. There are a total of 4 coil configurations which can provide dipole magnetic field for accelerators: cos-theta type [20], common coil type [21], block type [22] and canted cos-theta type [23]. Among these the common coil type is the simplest structure. The coils have much larger bending radius and there is much less strain level in the coils. Since both $Nb_3Sn$ and HTS superconducting materials are strain-sensitive, which means the critical current density $J_c$ of superconductors will be largely reduced by the high strain level, the common coil configuration has been chosen as the first option for the design study of the SPPC dipole magnets. A conceptual design study of the 12-T 2-in-1 dipole magnets is ongoing with the Iron-based superconducting (IBS) technology. The study is carried out with an expected $J_e$ level of IBS in 10 years, i.e., about 10 times higher than the present level, as shown in Figure 5 [24]. Besides the significant improvement of $J_e$, we are also expecting that the IBS superconductor would have much better mechanical performance comparing with present high field conductors like $Nb_3Sn$ and Bi-2212, and the much lower cost than them.

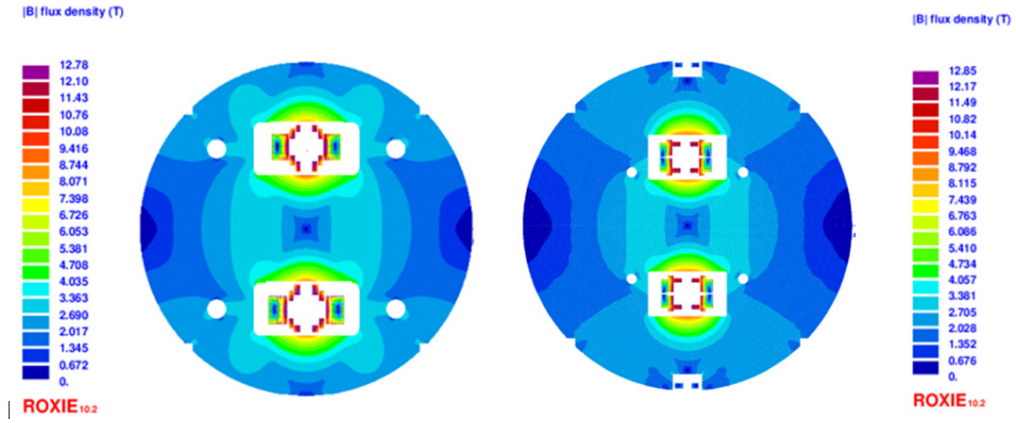


**Figure 6**: Field distribution of the design 1 (left) and design 2 (right).

The aperture diameter of the magnets is 45 mm. The main field is 12 T in the two apertures per magnet with $10^{-4}$ field uniformity. Two types of coil ends are considered and compared for the field quality and structure optimization: soft-way bending and hard-way bending. For the hard-way bending the coil is wound with flared ends and in such way the needed amount of superconductors is minimized. Study of two coil layouts have been completed, as shown in Figure 6. The main parameters of the magnets are listed in Table 1. The minimum bending radius of the cables is around 80 mm. The outer diameter of the magnet is temporarily set to 620 mm and the inter-aperture spacing is 236-258 mm. For design 1, we put 4 coil blocks with 8 turns per block in the inner two layers, 4 coil blocks with 21 turns per block in the middle and outside. With a current of 9400 A, we can get 12 T main field in the aperture and 12.78 T peak field in coils. For design 2, there are 4 coil blocks with 4 turns per block in the inner two layers, 2 coil blocks with 33(16+17 for gap) turns per block in the middle and 2 coil blocks with 28(14+14) turns per block in the outside. We can get a 12 T main field and 12.85 peak field with a current of 8100 A. Field distributions of the two designs are shown in Fig. 6. The operating margin is 21% at 4.2 K for the two designs.

As shown in Fig 7, for design 1, we choose to bend the upper two blocks in hard-way to save conductors and make space for beam pipes. Hard-way bending parts are on an ellipsoid with 5 degree of inclination angle to decrease the influence to field quality. For design 2, we bend all the coil blocks in soft-way. By optimizing lengths of coil straight sections one can achieve a $10^{-4}$ integrated field quality along axis. Fig. 8 shows field harmonics variation along axis for the design 2.

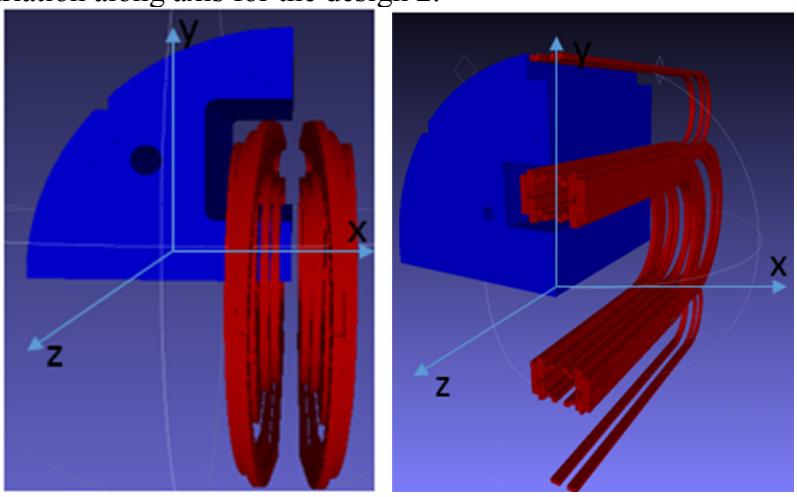


**Figure 7**. Left: the layout of hard-way coil ends. Right: the layout of soft-way coil ends

Table 1. Main parameters of the 12-T iron-based dipole magnet

| Parameter | Unit | Value |
|---|---|---|
| Number of apertures | - | 2 |
| Aperture diameter | mm | 45 |
| Inter-aperture spacing | mm | 236/258 |
| Operating current | A | 9400/8100 |
| Operating temperature | K | 4.2 |
| **Load line ratio** | / | 79% |
| Main field in the aperture | T | 12 |
| Coil peak field | T | 12.78/12.85 |
| Number of iron-based coils | - | 6 |
| Outer diameter of the magnet | mm | 620 |
| Minimum bending radius | mm | 85/77 |

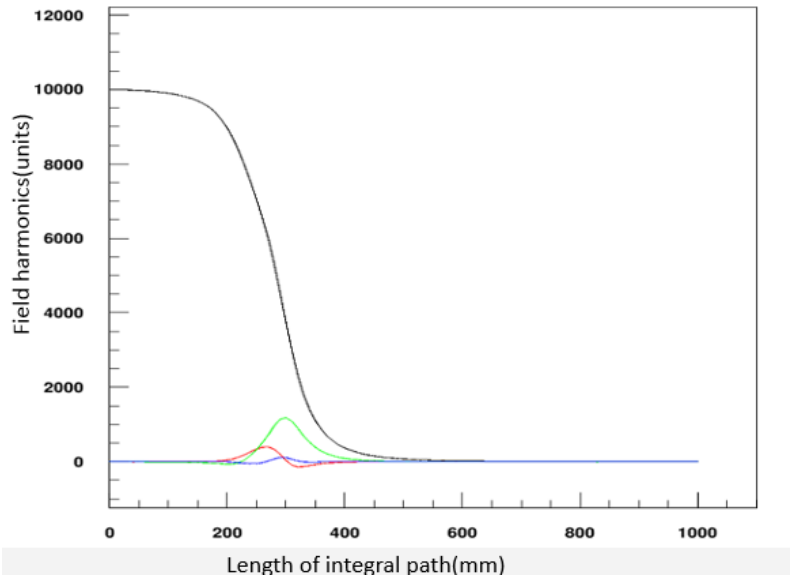


**Figure 8**. Field harmonics variation along axis for the design 2# (Black line stands for $b_1$, green line for $b_3$, red line for $b_5$, and blue line for $a_2$).

### 2.18.4 References


1. Y. Kamihara, T. Watanabe, M. Hirano, and H. Hosono, *J. Am. Chem. Soc.* **130**, 3296 (2008).
2. H. Hosono, K. Tanabe, E. Takayama-Muromachi, H. Kageyama, S. Yamanaka, H. Kumakura, M. Nohara, H. Hiramatsu, and S. Fujitsu, *Sci. Technol. Adv. Mater.* **16**, 033503 (2015).
3. A. Gurevich, *Rep. Prog. Phys.* **74**, 124501 (2011).
4. T. Katase, Y. Ishimaru, A. Tsukamoto, H. Hiramatsu, T. Kamiya, K. Tanabe, and H. Hosono, *Nat. Commun.* **2**, 409 (2011).
5. Y. W. Ma, *Supercond. Sci. Technol.* **25**, 113001 (2012).
6. J. D. Weiss, C. Tarantini, J. Jiang, F. Kametani, A. A. Polyanskii, D. C. Larbalestier, and E.E. Hellstrom, *Nat. Mater.* **11** 682 (2012).
7. S. Pyon, T. Suwa, A. Park et al. *Supercond. Sci. Technol.* **29**, 115002 (2016).
8. Z. Gao, K. Togano, A. Matsumoto, and H. Kumakura, Sci. Rep. **4** 4065 (2014).
9. X. P. Zhang, C. Yao, H. Lin, Y. Cai, Z. Chen, J. Q. Li, C. H. Dong, Q. J. Zhang, D. L. Wang, Y. W. Ma, H. Oguro, S. Awaji, and K. Watanabe, *Appl. Phys. Lett.* **104**, 202601 (2014).
10. H. Huang, C. Yao, C. H. Dong, X. P. Zhang, D. L. Wang, Z. Cheng, J. Q. Li, S. Awaji, and Y.W. Ma, arXiv:1705.09788 (2017)
11. F. Liu, C. Yao, H. Liu et al. *Supercond. Sci. Technol.* **30**, 07LT01 (2017).
12. C. Yao, Y. W. Ma, X. P. Zhang, D. L. Wang, C. L. Wang, H. Lin, and Q. J. Zhang, *Appl. Phys. Lett.* **102**, 082602 (2013).
13. K. L. Lin, C. Yao, X. P. Zhang, *et al. Supercond. Sci. Technol.* **29**, 095006 (2016).
14. Y. W. Ma, *Physica C* **516**, 17 (2015).
15. X. P. Zhang, H.Oguro, C. Yao, C. H. Dong, Z. T. Xu, D. L. Wang, S. Awaji, K. Watanabe, and Y. W. Ma, *IEEE Trans. Appl. Supercond.***27**, 7300705 (2017).
16. E. Kong et. al., Conceptual Design Study of Iron-based Superconducting Dipole Magnets for SPPC, to be published.

17. Q. Xu et. al., 20-T Dipole Magnet with Common Coil Configuration: Main Characteristics and Challenges, IEEE Trans. Appl. Supercond., VOL. 26, NO. 4, 2016, 4000404.
18. A. Greene et al., "The Magnet System of the Relativistic Heavy Ion Collider (RHIC)", IEEE Trans. Mag., VOL. 32, NO. 4, JULY 1996, pp 2041-2046.
19. LHC design report: The LHC Main Ring, Chapter 7: Main Magnets in the Arcs, [Online]. Available: http://ab-div.web.cern.ch/ab-div/Publications/LHC-DesignReport.html.
20. Alvin Tollestrup, Ezio Todesco, "The Development of Superconducting Magnets for Use in Particle Accelerators: From the Tevatron to the LHC," Reviews of Accelerator Science and Technology 04/2012; 01(01). DOI: 10.1142/S1793626808000101.
21. R. Gupta, "A Common Coil Design for High Field 2-in-1 Accelerator Magnets," Proceedings of the 1997 Particle Accelerator Conference, Vol. 3, May 1997, pp. 3344-3346.
22. Sabbi G et al., "Design of HD2: a 15 Tesla Nb3Sn dipole with a 35 mm bore," IEEE Trans. on Appl. Supercond. 15, 2005, pp 1128-1131.
23. S. Caspi et al., "Canted–Cosine–Theta Magnet (CCT)—A Concept for High Field Accelerator Magnets", IEEE Trans. on Appl. Supercond., VOL. 24, NO. 3, JUNE 2014 4001804
24. Peter Lee, Engineering Critical Current Density vs. Applied Field, https://nationalmaglab.org/magnet-development/applied-superconductivity-center/plots

## 2.19 HE-LHC Overview, Parameters and Challenges

Frank Zimmermann
CERN, Route de Meyrin, 1211 Geneva 23, Switzerland

Mail to: frank.zimmermann@cern.ch

### 2.19.1 Introduction

In the frame of the Future Circular Collider (FCC) study [1], the FCC collaboration is designing a 27 TeV hadron collider installed in the existing LHC tunnel, called the High Energy LHC (HE-LHC). The HE-LHC shall be realized by replacing the LHC's 8.33 Tesla Nb-Ti dipole magnets with 16 Tesla $Nb_3Sn$ magnets being developed for the 100 TeV hadron collider FCC-hh [1,1].

We note that this new version of the HE-LHC differs from the HE-LHC studied in the year 2010 [3,4], which featured a higher centre-of-mass energy of 33 TeV (based on 20 Tesla hybrid magnets also containing high-temperature superconductor), along with a reduced beam current, and lower luminosity.

### 2.19.2 Design Targets and Constraints

The HE-LHC physics goals call for a doubling the LHC collision energy, which can be achieved with the help of FCC-hh magnet technology, i.e. by replacing the existing